Long-term tectonic control on Holocene shelf sedimentation offshore La Jolla, California

Leah J. Hogarth*
Jeffrey Babcock
Neal W. Driscoll
Nicolas Le Dantec
Jennifer K. Haas
Douglas L. Inman
Patricia M. Masters
Scripps Institution of Oceanography, University of California–San Diego, La Jolla, California 92093, USA

ABSTRACT

A high-resolution Compressed High-Intensity Radar Pulse (CHIRP) survey reveals shore-parallel variations in the Holocene sediment thickness offshore La Jolla, California. Sediment thicknesses decrease from >20 m in the south near Scripps Canyon to zero in the north approaching Torrey Pines. In addition to the south-to-north variation in sediment thickness, the transgressive surface observed in seismic lines shoals from Scripps Canyon to the north. Despite these dramatic shore-parallel subsurface changes, the nearshore bathymetry exhibits little to no change along strike. A left jog (i.e., a constraining bend) along the Rose Canyon fault causes local uplift in the region and appears to explain the northward shoaling of the transgressive surface, the decrease in relief on the transgressive surface away from the left jog, and the Holocene sediment thickness variation. This tectonic deformation is shore parallel, and thus the accommodation can be separated into its tectonic and eustatic components.

Keywords: tectonic deformation, accommodation, transgressive surface, transpression.

INTRODUCTION

Many investigators have recognized the important role of tectonics in the preservation of sediments on active margin shelves (e.g., Orange, 1999; Driscoll and Hogg, 1995). In most locations, tectonic uplift or subsidence offsets the coastline vertically and causes base-level changes that are difficult to distinguish from sea-level changes; a common manifestation of tectonic uplift is subaerial terraces parallel to the coastline. Eustatic sea level has risen ~125 m in the past 20 k.y. (e.g., Fairbanks, 1989). Consequently, in seismic images and in outcrop, it is often difficult to separate sea-level changes from tectonic changes acting in the same plane during this time period. In the San Diego, California, area, regional uplift and sea-level change have created terraces (e.g., Bay Point Formation), but due to the geometry of the Rose Canyon fault zone, much tectonic deformation occurs shore parallel or orthogonal to eustatic sea-level changes and regional tectonic uplift (Kennedy, 1975). Thus, we can use the stratigraphic variability parallel to shore to discern the tectonic signal associated with the Rose Canyon fault from glacial-eustatic fluctuations or regional tectonic uplift. Furthermore, this will aid us in understanding how tectonic processes govern the preservation of sediments on the shelf. Such an understanding will allow us to define sand resources offshore as well as the distribution of hardgrounds on the seafloor, which may play an important role in biohabitats.

The San Diego area is west of the San Andreas fault zone and is characterized by a series of subparallel, en echelon faults including, from east to west, the San Jacinto, Elsinore, and Newport–Inglewood–Rose Canyon fault zones. In the La Jolla region, the Rose Canyon fault zone is a dextral strike-slip fault zone with complex surface expression (Treiman, 1993). The fault zone passes through La Jolla, forming Mount Soledad, a pop-up structure with a maximum uplift of ~150 m (Fig. 1); pop-up structures are areas of local uplift due to transpression or compression created when lateral motion on a strike-slip fault is interrupted by a bend or a jog in that fault. In the case of Mount Soledad, a left-stepping jog on the right-lateral Rose Canyon fault creates compression and uplift (Kennedy, 1975; Kennedy et al., 1979). Seismic surveys reveal that the Rose Canyon fault zone extends northwest 60 km offshore (Moore, 1972). Evidence of Holocene activity on the Rose Canyon fault zone comes from both offshore seismic data (Moore, 1972) and onshore trenches (Lindvall and Rockwell, 1995). Lindvall and Rockwell (1995) estimated that the total horizontal component of slip ranges from 1 to 2 mm/yr during the Holocene. In addition to the Rose Canyon fault system, Kennedy (1975) identified several other inactive northeast-southwest–trending oblique faults with vertical offset of ~10 m in the cliffs of Torrey Pines Beach (Fig. 1).

Our objective is to image the transgressive surface, overlying sands, and fault structures to better understand the processes influencing sediment accumulation and preservation on the shelf near La Jolla. Here we describe the observed morphology of the transgressive surface. We propose that our observation of a pop-up structure offshore, created by a constraining bend along the right-lateral Rose Canyon fault zone, controls the long-term accumulation of sediment in this region of the nearshore.

METHODS

In 2002, ~300 km of Compressed High-Intensity Radar Pulse (CHIRP) seismic data were acquired offshore from La Jolla Cove north to Del Mar (Fig. 1). We used a CHIRP sonar (Edgetech) with a swept frequency of 1–5.5 kHz yielding submeter vertical resolution. During the nearshore survey, the CHIRP seismic system was mounted on a surface tow frame with an attached global positioning system receiver, thus minimizing navigation error. We generated an isopach map by tracing the transgressive surface and differencing it from the seafloor throughout the seismic grid. A nominal velocity of 1500 m/s was used to convert travel-

*E-mail: lhogarth@ucsd.edu.

time to sediment thickness. Bathymetric data were acquired, processed, archived, and distributed by the Seafloor Mapping Lab of California State University Monterey Bay (http://seafloor.csumb.edu/SFMLwebDATA.htm).

RESULTS

Layers in the units below the transgressive surface generally exhibit distinct dips to the south (Fig. 2) that are consistent with the local dips of the Ardath Shale, Torrey Sandstone, and Del Mar Formation on land (Kennedy, 1975). The transgressive surface is identified in the profiles by marked truncation (Figs. 2 and 3), which was formed by wave-base erosion during the sea-level rise, and is mantled by a basal unit and an overlying acoustically transparent layer. This part of the shelf has been subaerially exposed during many sea-level lowstands during the Pleistocene; the erosion and truncation on this surface probably reflect multiple sea-level cycles, not just the last sea-level rise. The poorly laminated basal unit is only observed in the mid- to outer-shelf region and appears to record the early transgression in the region. The overlying transparent unit might reflect the early stage of the highstand systems tract, which exhibits cross-shelf thinning with a maximum depocenter in the mid-shelf. The acoustically transparent character, however, precludes identification of a downlap surface, and thus our ability to confidently discern whether this package is part of the late transgressive systems tract or the early highstand systems tract.

Seismic images from our survey show that the transgressive surface exhibits an overall southward dip, and the overlying sediment thickness decreases along strike to the north of Scripps Canyon (Figs. 2 and 4). A local reversal of dip also exhibits a change in acoustic reflectivity that might imply a more resistive hardground and may be fault controlled (Fig. 2A). It is difficult, however, to trace the fault laterally shoreward from line S10 to adjacent lines because of the limited acoustic penetration beneath the transgressive surface (Fig. 2A). The dip lines show that the maximum sediment thickness above the transgressive surface is located on the mid-shelf and systematically diminishes both landward and seaward (Fig. 3). The extent of the isopach map is limited by data density; it captures the edge of the mid-shelf depocenter and delineates the south-to-north thinning.

The isopach map of sediment thickness shows a depocenter between the La Jolla and Scripps canyons, as well as to the north of Scripps Canyon (Fig. 4). Sediment thickness systematically decreases along strike to the north from ~20 m just north of Scripps Canyon to zero offshore Torrey Pines (Figs. 2 and 4). Perpendicular to shore, sediment thickness ranges from ~0–5 m nearshore to maximum thicknesses of 10–20 m

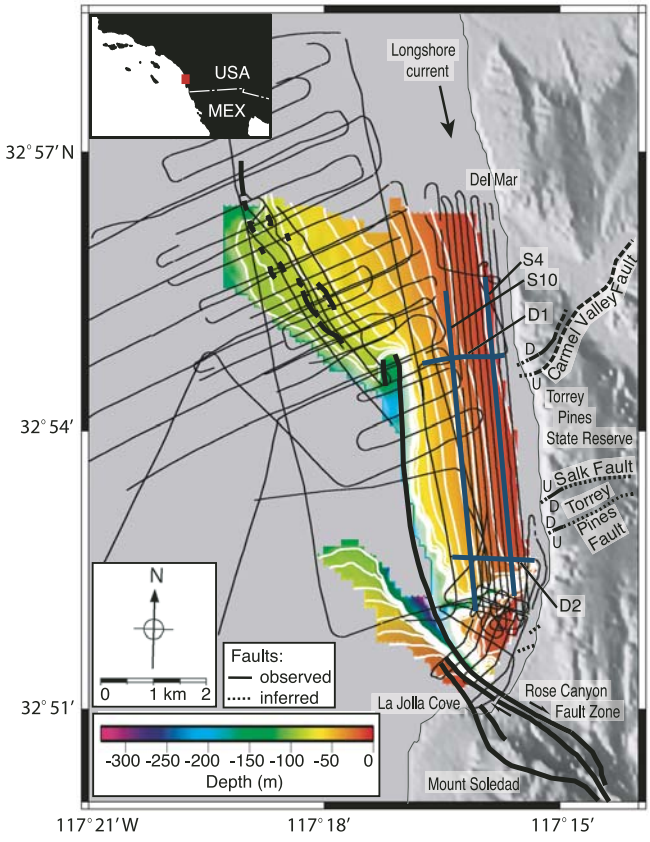

Figure 1. Survey ship track (black lines) superimposed on 2 m gridded bathymetry (data used in this study were acquired, processed, archived, and distributed by Seafloor Mapping Lab of California State University Monterey Bay: http://seafloor.csumb.edu/SFMLwebDATA.htm). White lines on bathymetry are contours (10 m intervals) to 100 m. Faults are shown in bold black: dashed for inferred location, D and U for downthrown and upthrown side, and right-lateral sense of strike-slip motion is shown with arrows. Left-stepping bend in Rose Canyon fault zone creates uplift of Mount Soledad. S4, S10, D1, and D2 (bold blue lines) indicate locations of strike lines shown in Figure 2 and dip lines shown in Figure 3. Local faults shown are based on Kennedy (1975).

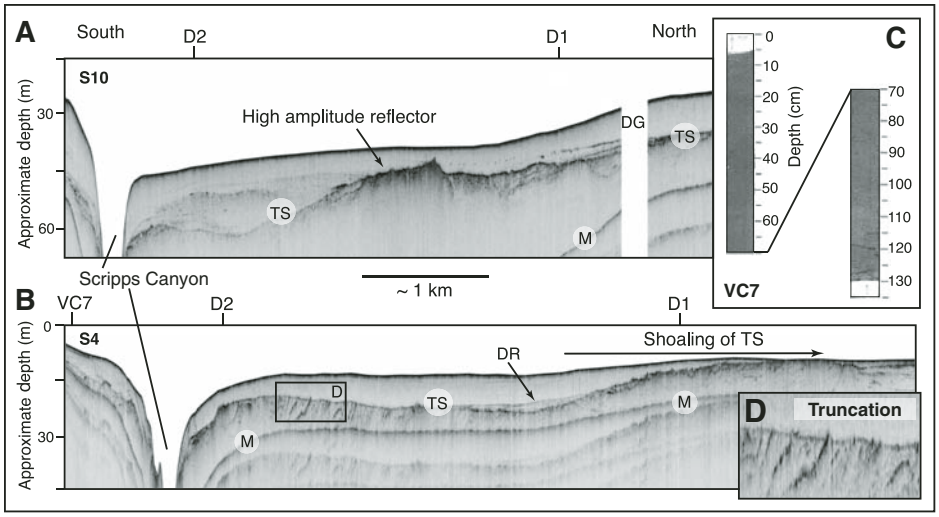

Figure 2. CHIRP along-shelf strike lines. A: Profile S10 from offshore shows shoaling of transgressive surface (TS) to north of Scripps Canyon. At this depth, Holocene sediments mantle transgressive surface. B: Nearshore profile S4 shows truncation of underlying layers as consequence of wavebase erosion, which is interpreted to occur during sea-level transgression. TS is exposed at seafloor to north. Vibracore VC7 is projected onto line S4 south of Scripps Canyon. D1 and D2 are locations of crossing dip lines. See Figure 1 for locations (M—multiple, DG—data gap, DR—dipping reflector). C: Inset shows Vibracore VC7, which recovered fine-grained to very fine grained, olive-green, homogeneous sands. In upper 135 cm of Holocene sediment there is no evidence for event beds associated with storms or floods. See Figure 4 for core location. D: Inset shows detail of TS and associated truncation.

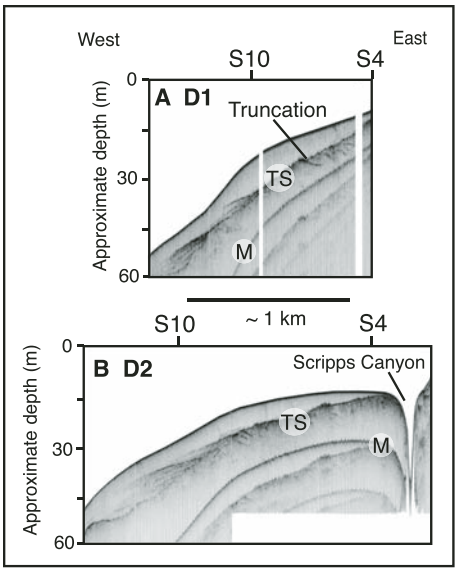

Figure 3. CHIRP cross-shelf dip lines. A: Profile D1 shows truncation along interpreted transgressive surface. Basal reflective package is interpreted as part of early transgression, and thickness of overlying acoustically transparent unit is greatest in mid-shelf, thinning both landward and seaward. B: Profile D2, farther to south, also shows mid-shelf depocenter of acoustically transparent unit. S4 and S10 are locations of crossing strike lines. TS—transgressive surface; M—multiple. See Figure 1 for locations.

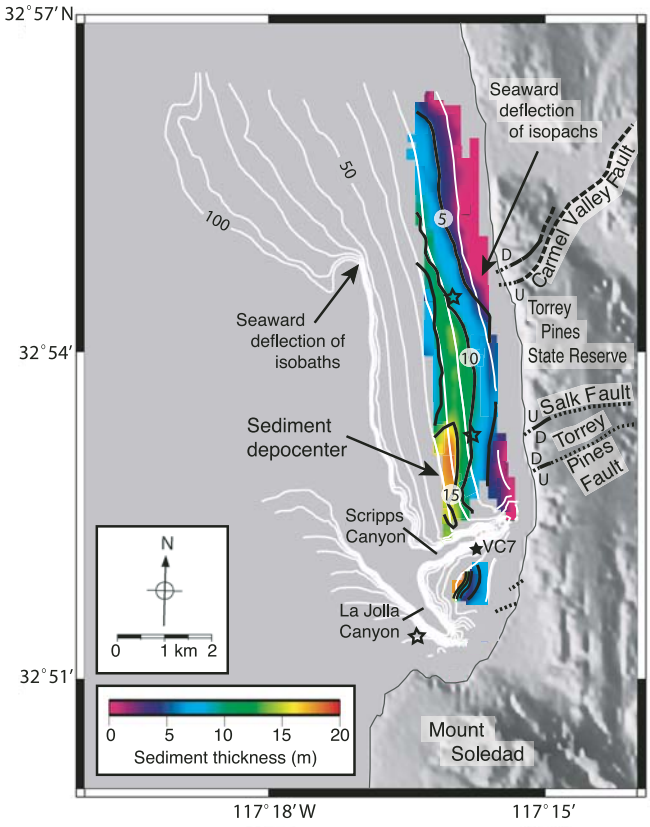

Figure 4. Holocene sediment thickness above transgressive surface (contour interval = 5 m) superimposed on bathymetric contours (contour interval = 10 m). Extent of isopach map is limited to mid-shelf and shoreward by data density shown in Figure 1. Isopachs show depocenter of Holocene sediments directly north of Scripps Canyon, where sediments are nearly 20 m thick. Along strike to the north, sediments thin to zero, whereas bathymetry does not change. Note spatial correlation between the step offshore of isobaths >60 m and that of isopachs. Stars represent locations of Vibracores; solid for this study (2005) and unfilled for previous study (Darigo and Osbourne, 1986).

in the mid-shelf region before thinning again as water depth increases (Figs. 3 and 4).

The area where hardgrounds crop out to the north correlates with the deflection of bathymetric contours offshore at water depths >60 m (Fig. 4). Note that the nearshore contours do not exhibit this deflection, even though the slope of the isopach surface changes in this area from west dipping to southwest dipping.

A 135-cm-long Vibracore acquired in 2005 (Figs. 2 and 4) recovered fine-grained to very fine grained, olive-green, homogeneous sands consistent with the sediment recovered in longer Vibracores from the region (Darigo and Osbourne, 1986; Fig. 4). Mud horizons or coarse layers indicative of flood or storm events are not observed in this homogeneous upper layer. Beneath the sand is a slightly coarser unit that is not as well sorted, and includes larger clasts and more abundant shell fragments (units II and III of Darigo and Osbourne, 1986), which may be a transgressive lag deposit. The major fluvial input to this littoral cell is by the Santa Margarita and San Luis Rey rivers to the north, with predominant southern longshore transport (Inman and Jenkins, 1999). Wave reworking and longshore transport winnow out the fine-grained particles, resulting in a homogeneous nearshore deposit, consistent with the transparent acoustic character observed in the seismic data. Early Holocene floods may have contributed coarser material, but fine-grained to very fine grained sand likely resulted from the past 5 k.y. of enhanced El Niño–driven wave energy and consequent southern sand transport (Masters, 2006).

DISCUSSION

Several faulting trends in the La Jolla area could potentially explain the observed seafloor structure and sediment distribution. For example, one possible scenario is that the relief on the transgressive surface is only controlled by steeply dipping northeast-southwest–trending normal faults, such as those observed onshore at the southern end of Torrey Pines State Reserve (e.g., Carmel Valley fault, Fig. 1). On the basis of terrace offsets, these faults are older than 120 ka (Treiman, 1993). If such a fault caused uplift of the more resistant Del Mar Formation to the north with respect to the less resistant Scripps Formation to the south, we would expect a jog of isobaths seaward as the more resistant Del Mar Formation formed a promontory. If this scenario were correct, it would not predict that the isobaths should return shoreward north of the fault (Fig. 5A), and the faults would cause a marked local thickness change across the fault from the downdropped to the upthrown block (e.g., Fig. 2A). The lateral extent of the depocenter exhibits a wavelength longer than that of the onshore downdropped block bounded by the Salk and Torrey Pines faults (Figs. 1 and 4). Furthermore, the Carmel Valley fault onshore is down to the north; i.e., the sense of motion across the fault is opposite to that predicted by the observed sediment thickness. Alternatively, in a pop-up or constraining bend scenario, a left jog in a right-lateral fault zone would cause the thickness of the transgressive deposits to thin systematically from the depocenter toward the structural high without a sharp local thickness change (Fig. 5B). Such a constraining bend would predict that the isobaths shift seaward at the south end and return shoreward at the north end of the pop-up structure, which is consistent with the isobaths deeper than ~60 m (Fig. 4; see also the regional National Oceanic and Atmospheric Administration (NOAA) National Geophysical Data Center 3-arc-second coastal relief model [http://www.ngdc.noaa.gov/mgg/coastal/grddas06/grddas06.htm]). A gentle, long-wavelength uplift of the transgressive surface is observed in the seismic images, consistent with a left jog along the Rose Canyon fault zone. The relief on the transgressive surface is largest in the west near the jog in the Rose Canyon fault (e.g., 26.5 m; Fig. 2A) and diminishes eastward away from the jog (e.g., 21.5 m; Fig. 2B), as would be predicted by the pop-up hypothesis (Fig. 5). Seismic data recently acquired (2005 R/V *New*

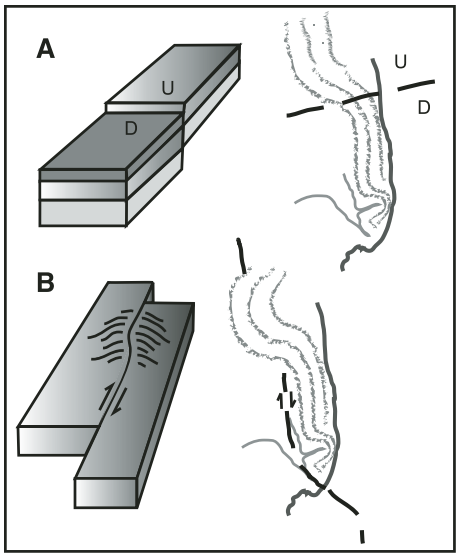

Figure 5. Two models of possible faulting mechanisms and expected bathymetry. A: Offset with more resistant Del Mar Formation exposed on upthrown block, along predominantly strike-slip fault, would cause bathymetry to step offshore. B: In case of left step on dextral strike-slip fault (e.g., Rose Canyon fault), we would expect bathymetric contours to deviate seaward on south end of fault and return landward on north end of fault, which we observe in both local bathymetry (California State University Monterey Bay 2 m) and regional bathymetry (National Oceanographic and Atmospheric Administration 3-arc-second model: http://www.ngdc.noaa.gov/mgg/coastal/grddas06/grddas06.htm). Black lines indicate fault trace; sense of motion is illustrated by arrows or D and U for downthrown and upthrown blocks.

Horizon cruise, unpublished data) to the north of the pop-up structure, where the isobaths shift shoreward, reveal that the transgressive surface has a northward dip, which is also consistent with the pop-up model. The relief on this surface may be augmented by the differential erodibility of the Eocene subsurface rocks, more indurated in the north than in the south (Kennedy, 1975).

The thickness of sediments between the canyons and directly north of Scripps Canyon, along with the near absence of sediments on the structural high to the north, suggest that uplift along constraining bends of the Rose Canyon fault plays an important role in long-term sediment accumulation in the region. The relief on the transgressive surface that predates sea-level incursion is difficult to constrain, and thus prevents reliable estimates for the deformation rate after sea-level incursion. Any relict relief would have created promontories and embayments. The dip of the reflector (DR) overlying the transgressive surface observed in line S4 can be explained by either post-transgression tilting or as backfill associated with erosion of the relict promontory (Fig. 2B). If we assume that all the relief postdates the sea-level rise, the estimated uplift rate will be biased toward a maximum. For example, if this differential relief is the consequence of tectonic uplift and tilting since inundation (ca. 10 ka), it yields deformation rates an order of magnitude larger than previous estimates of uplift rate in the region (0.13–0.14 mm/yr; Legg and Kennedy, 1979). Given that it is difficult to determine what portion of the relief is pre-incursion or post-incursion, long cores are required to place further constraints on the local tectonic uplift rates.

CONCLUSIONS

High-resolution geophysical data suggest that uplift offshore La Jolla, California, results from a left jog along the Rose Canyon right-lateral fault system, similar to the process responsible for forming Mount Soledad onshore. CHIRP seismic profiles show a shoaling of the transgressive surface from south to north. The seaward deflection of isobaths in the bathymetric data correlates with the change in slope of the transgressive surface and the change in overlying sediment thickness observed in the isopach map. Seismic profiles reveal that the sediments thin to zero above the uplifted bedrock, while the thickest sediments occur to the south of the pop-up structure. The observed sediment thicknesses suggest that tectonics control long-term sediment accumulation in the region, and hydrodynamics control sediment dispersion. Strain accommodation between right-lateral fault segments offshore Southern California results in marked thickness variability of the Holocene sediments. This new insight into controls on sediment accumulation and preservation may advance the understanding of our offshore sand resources and exposure of hardgrounds in the California Borderlands.

ACKNOWLEDGMENTS

This research was funded by the Office of Naval Research and the Kavli Institute. Reviews from Paul Liu, Dan Orange, and Glen Spinelli improved the manuscript.

REFERENCES CITED

Darigo, N.J., and Osbourne, R.H., 1986, Quaternary stratigraphy and sedimentation of the inner continental shelf, San Diego County, California, *in* Knight, R.J., and McLean, J.R., eds., Shelf sands and sandstones: Canadian Society of Petroleum Geologists Memoir II, p. 73–98.

Driscoll, N.W., and Hogg, J.R., 1995, Stratigraphic response to basin formation; Jeanne d'Arc Basin, offshore, Newfoundland, *in* Lambiase, J.J., ed., Hydrocarbon habitat in rift basins: Geological Society of London Special Publication 80, p. 145–163.

Fairbanks, R.G., 1989, A 17,000-year glacio-eustatic sea level record: Influence of glacial melting rates on the Younger Dryas event and deep-ocean circulation: Nature, v. 342, p. 637–642, doi: 10.1038/342637a0.

Inman, D.L., and Jenkins, S.A., 1999, Climate change and the episodicity of sediment flux of small California rivers: Journal of Geology, v. 107, p. 251–270, doi: 10.1086/314346.

Kennedy, M.P., 1975, Western San Diego metropolitan area; Del Mar, La Jolla, and Point Loma 7 1/2 minute quadrangles: California Division of Mines and Geology Bulletin, v. 200, p. 9–39.

Kennedy, M.P., Clarke, S.H., Greene, H.G., and Legg, M.R., 1979, Recency and character of faulting offshore from metropolitan San Diego, California: California Division of Mines and Geology, 37 p.

Legg, M.R., and Kennedy, M.P., 1979, Faulting offshore San Diego and northern Baja, California, *in* Abbott, P.L., and Elliott, W.J., eds., Earthquakes and other perils, San Diego region: San Diego, California, San Diego Association of Geologists, p. 29–46.

Lindvall, S.C., and Rockwell, T.K., 1995, Holocene activity of the Rose Canyon fault zone in San Diego, California: Journal of Geophysical Research B, Solid Earth and Planets, v. 100, p. 24,121–24,132, doi: 10.1029/95JB02627.

Masters, P.M., 2006, Holocene sand beaches of southern California: ENSO forcing and coastal processes on millennial scales: Palaeogeography, Palaeoclimatology, Palaeoecology, v. 232, p. 73–95, doi: 10.1016/j.palaeo.2005.08.010.

Moore, G.W., 1972, Offshore extension of the Rose Canyon fault, San Diego, California: U.S. Geological Survey Professional Paper P 0800-C, p. 113–116.

National Oceanic and Atmospheric Administration (NOAA) National Geophysical Data Center (NGDC) 3-arc-second coastal relief model: http://www.ngdc.noaa.gov/mgg/coastal/grddas06/grddas06.htm (July 2006).

Orange, D.L., 1999, Tectonics, sedimentation, and erosion in northern California; Submarine geomorphology and sediment preservation potential as a result of three competing processes; The formation of continental-margin strata: Marine Geology, v. 154, p. 369–382, doi: 10.1016/S0025–3227(98)00124–8.

Treiman, J.A., 1993, The Rose Canyon fault zone, southern California: California Division of Mines and Geology Open File Report 93–02, 45 p.

Manuscript received 25 July 2006
Revised manuscript received 21 October 2006
Manuscript accepted 29 October 2006

Printed in USA